Experimental study of the bed morphology downstream of a sluice gate

Luís Carvalho[1], *Elsa* Carvalho[2], *Rui* Aleixo[3], and *Maria Manuela* C. L. Lima[1,*]

[1]Escola de Engenharia da Universidade do Minho, Campus de Azurém, 4800-058 Guimarães, Portugal
[2]Faculdade de Engenharia, Universidade do Porto, Rua do Sr. Roberto Frias s/n, 4200-465 Porto, Portugal
[3]University of Bologna, Via del Lazzaretto 15/5, 40126 Bologna, Italy

Abstract. This work describes an experimental study based on a simplified model of a vertical sluice gate installed in a channel with a moving bed of glass spheres with 2 mm diameter. The originated scour cavity and downstream dune were studied. The influence of the apron length and the downstream tailwater depth were also analysed. Imaging techniques provided the tools to this investigation. The data acquisition and processing consisted in acquiring images of the flow and automatically process them to identify the water-sediments interface and the longitudinal profile of sediments' bed at different instants.

1. Introduction

Scour can occur next to obstacles or due to the lateral contraction of the flow, and it is often associated with the collapse of hydraulic structures [1-3]. It is necessary to predict the maximum scour depth associated to hydraulic constructions such as sluice gates, to avoid accidents that could affect their stability and endanger human lives. Furthermore, the morphology of the river bed downstream is affected by scour and a dune or bar is formed, introducing severe changes in the flow and sediment transport [4].

The scour downstream of a sluice gate is originated by a turbulent submerged horizontal jet, usually considered to be two-dimensional [5]. The conjugation of sluice gate opening dimension, tail water depth, flow rate, as well as the existence of an apron results in different jets that can be accompanied by a hydraulic jump. The flow is highly turbulent, even for relatively low jet Froude numbers, and a scour cavity develops at different rates depending on the sediment size and its nonuniformity [6]. Besides the prevision of the maximum scour (e.g. [7]) that allows the correct design of such structures, the dune evolution downstream can provide insights into the sediment transport mechanism [4]. An extensive bibliographic revue of the flow under a sluice gate and its influence on scour can be found in [5-7].

This work aims at analysing this phenomenon in the case of an idealized sediment bed in a small channel, where experimental parameters can be easily established, and the flow can be considered bidimensional. A simple experimental procedure, based on video

* Corresponding author: mmlima@civil.uminho.pt

recording and image processing that allows the identification of the free water surface and the bed of sediments, was developed.

2. Experimental setup and methodology

2.1. Experimental setup

The scour downstream a sluice gate was studied experimentally in a closed-circuit flume. This flume was 615 mm long, 150 mm deep and 15 mm wide. The flow was controlled by a gate valve and the established flow rate was determined volumetrically using a beaker with 5 mL resolution and a digital chronometer. The sluice gate height was set at b = 6 mm (Figure 1). Water depth (y_t) in the channel was controlled by a vertical weir (of height p) at the downstream extremity of the flume. The bottom of the flume consisted of an apron with variable length (L) between 0 and 100 mm. Downstream the apron there was a sediment box (62 mm deep) filled in with 2 mm diameter glass spheres. This kind of idealized sediment bed was adopted to neglect the effect of sediment nonuniformity. Due to the small transversal dimension of the flume the sediment bed morphology could be easily visualized and monitored with a video camera. The sediment size allowed the bed of particles to be well identified in the images, resulting in a clear definition of the sediment-water interface during the experiments. Image processing was performed allowing the identification of the bed longitudinal profiles after the scour process had begun.

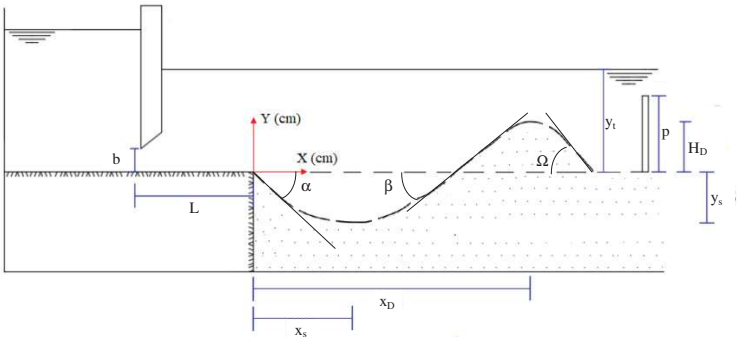

Fig. 1. Test section. y_s is the maximum scour depth and x_s is the corresponding x coordinate. H_D is the maximum dune height and x_D is the corresponding x coordinate. α and β are the upstream and downstream slopes of the scour cavity, respectively. Ω is the downstream slope of the dune.

2.2. Tested conditions

Table 1 lists the experiments carried out. The jet Froude number (equation 1), based on the sluice gate opening and jet mean velocity (U_j), was approximately equal to 3.9. The corresponding flow Froude number (equation 2), based on the tailwater depth (y_t) and downstream flow mean velocity (U), varied between 0.18 and 0.36. The densimetric Froude number (equation 3), based on the glass spheres diameter (D) and density (s), varied between 5.33 and 5.39. The tailwater depth of a free jump (y_j) (equation 4) allowed the calculation of the submergence ratio (equation 5).

$$Fr_b = \frac{U_j}{\sqrt{gb}} \tag{1}$$

$$Fr_p = \frac{U}{\sqrt{g y_t}} \tag{2}$$

$$Fr_d = \frac{U_j}{\sqrt{(s-1)gD}} \tag{3}$$

$$y_j = 0.5\, b \left(\sqrt{1 + 8Fr_b^2} - 1\right) \tag{4}$$

$$S = \frac{y_t - y_j}{y_j} \tag{5}$$

Table 1. Experimental conditions tested.

N.	Q (10^{-3} Ls^{-1})	b (cm)	L (cm)	p (cm)	y_t (cm)	y_j (cm)	Fr_b	Fr_p	Fr_d	S
1	85	0.6	0	1	3.09	3.02	3.89	0.33	5.33	0.02
2	86	0.6	0	2.5	4.55	3.06	3.94	0.19	5.39	0.49
3	85	0.6	8	1	3.09	3.02	3.89	0.33	5.33	0.02
4	85	0.6	8	2.5	4.69	3.02	3.89	0.18	5.33	0.55

2.3. Procedure

This subsection describes the experimental procedure adopted for the experiments and the analysis of the configuration of the bed of sediments. The spheres were carefully placed inside the channel and the spheres' bed was levelled. Water was added, and care was taken to ensure that the air inside the sediment bed was removed, by mixing the bed with a small rod. After levelling the surface of the glass spheres, the flume was filled with water until the defined water level and flow rate were reached. The video recording, by means of a video camera Sony HDR-XR105E Full HD 1080, was initiated with the filling of the flume. The initial instant of the experiments (t = 0 s) is the instant when the sluice gate is placed inside the flume. This instant is also recorded. The experiments duration ranged between 8 and 14 minutes, and it was determined by the fact that no changes in the sediment bed were observed.

The focal distance and aperture of the video camera was the same for all conditions. The images were acquired with a frequency of 24 fps. To convert pixels in physical units, a ruler placed in the bottom of the channel was used, together with the grid in the back window of the flume. To ensure an optimal contrast between water and sediments, care was taken with the test section lightning. Attention was given to avoid spurious light reflections and a black background was added to the setup.

For an efficient use of the camera's resolution, each experiment was carried out twice. In the first time the region near the sluice gate was filmed, and in the second time the experiment was repeated in the same conditions and the region corresponding to the second half of the flume was filmed (Figure 2). These regions overlapped 64 mm, so that afterwards the images could be stitched (Figure 3), thus increasing the overall field of view.

The videos were then converted into still images at pre-established instants and the images were processed to attain one full image of the flume. To process the images and to extract quantitative information, a code in Matlab was made. This code had two main parts. The first one was the stitching operation, where consecutive images were stitched together as shown in Figures 2 and 3. In this operation a correction for the lens distortion was also applied. The second part of the code was the filtering and boundary extracting. A gaussian filter was first applied to smooth the irregularities of the image, followed by a median filter to remove the noise. The bed is then highlighted by imposing a convenient threshold and

the Sobel edge-detector algorithm is then used to determine the boundary. The final result is depicted in Figure 4.

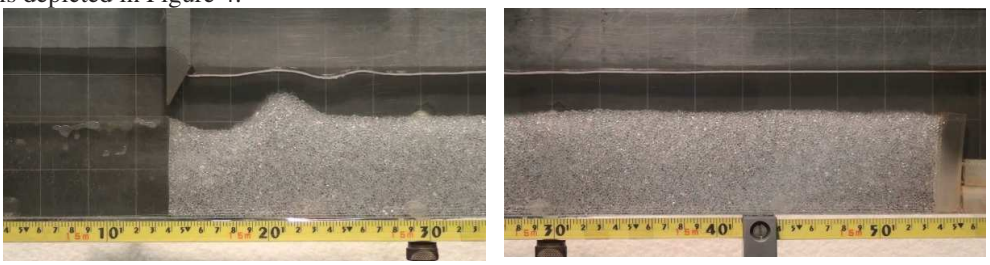

(a) (b)

Fig. 2. Images of the initial (a) and final (b) part of the channel, obtained for the experimental condition N. 1 at time t = 5 s.

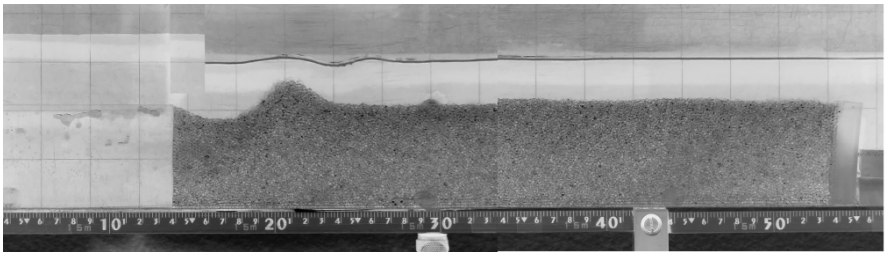

Fig. 3. Resulting full image, obtained for the experimental condition N. 1 at time t = 5 s.

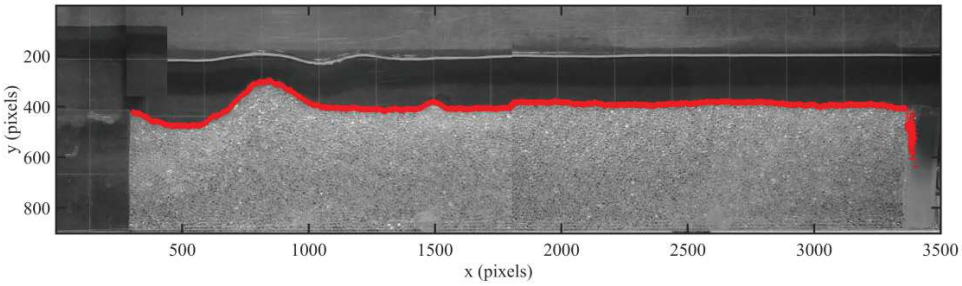

Fig. 4. Sediment-water interface recognition for the experimental condition N. 1 at time t = 5 s.

3. Results and discussion

Results show the time evolution of the scoured cavity profile for different flow conditions. The influences of the apron length and tail water depth were determined.

3.1. Time evolution of the sediment bed

In case of flow condition N.1 results (Figure 5) show that the scour cavity begins immediately after the sluice gate section (x = 0) and increases in depth and extension with time. The same behaviour was observed for the other tested conditions, however the obtained values of maximum scour depth, its location, maximum dune height and corresponding location vary accordingly to the experimental parameters (Table 1).

The point of maximum scour depth (Figure 6a) moves downstream with time (Figure 6b). The maximum scour depth increases at a higher rate in case of flow conditions N.1 andN.2, when compared to flow conditions N.3 and N.4. This behaviour is attributed to the fact that, in conditions N.1 and N.2, the jet issuing the sluice gate immediately contacts the sediment bed due to the inexistence of an apron ($L = 0$ cm). In case of $L = 8$ cm (conditions N.3 and N.4) the jet decelerates as it flows over the apron while a wall boundary layer develops, until it becomes fully developed. According to [7] a minimum length of 6 to 8 times the sluice gate opening is required to achieve fully developed flow. In the case of $L = 8$ cm, the corresponding apron's length is equal to 13.3 times the sluice gate opening, and hence the flow is considered to be developed.

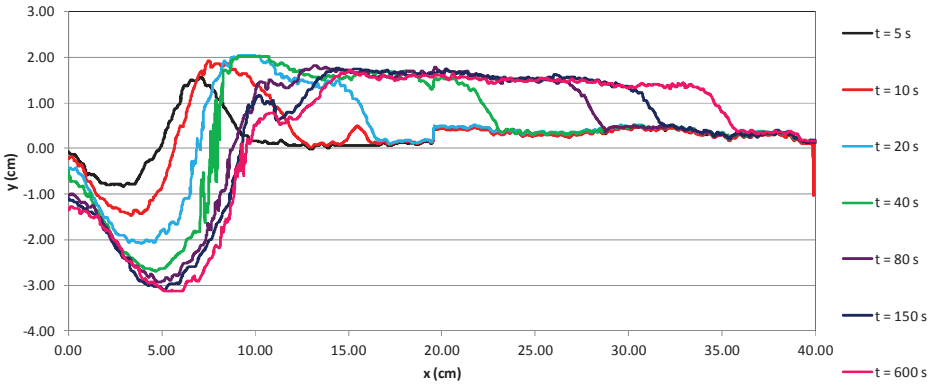

Fig. 5. Time evolution of the sediment bed in case of test condition N.1.

The maximum scour depth shows also the influence of the downstream tailwater depth, expressed by the parameter p. For shallower flows downstream the maximum scour depth is higher. This can also be justified by the fact that the submergence ratio of the jet is very small (≈ 0.02) in case of conditions N.1 and N.3, while for conditions N.2 and N.4 it is approximately equal to 0.5. Higher submergence ratios correspond to higher energy dissipation in the hydraulic jump that occurs downstream the sluice gate. The influences of the apron length and tailwater depth in the longitudinal position (x_s) of the maximum scour depth (Figure 7b) are not so pronounced, although the same overall pattern is observed.

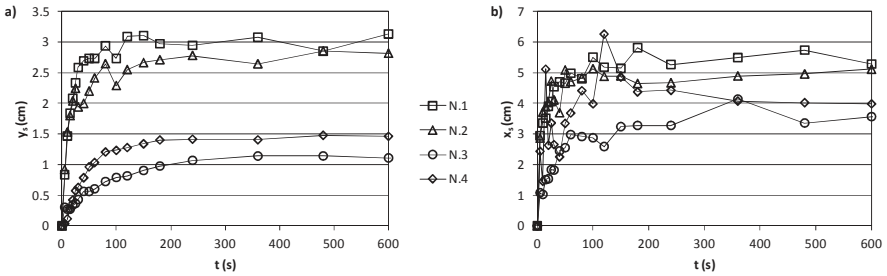

Fig. 6. Maximum scour depth evolution with time (a) and corresponding longitudinal position (b).

The eroded sediments accumulate in a dune or bar that forms downstream. This dune maximum height slightly increases with time (Figure 7a), as it migrates downstream (Figure 7b). For $t > 20$ s the crest of the dune becomes flat and the dune moves further downstream, while its maximum extension (roughly corresponding to the extension of the flat crest between the upstream and downstream slopes) increases. The maximum dune height increases at a higher rate in case of flow conditions N.1 and N.2, when compared to

flow conditions N.3 and N.4. For a fixed value of L, the dune height is higher for higher tailwater depths (N.2 and N.4), because in shallower flows the higher values of mean velocity and Fr_p contribute to the sediment transport and smoothing of the dune crest.

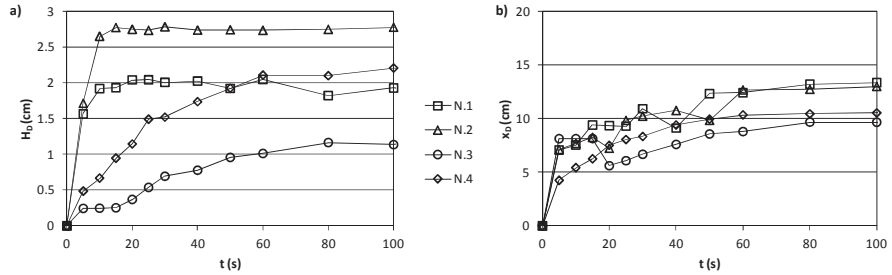

Fig. 7. Maximum dune height evolution with time (a) and corresponding longitudinal position (b). Only the first 100 s are presented since, afterwards, dune maximum height and location remain practically constant.

In order to evaluate the overall quality of the developed experimental method, the repeatability of the experiments was checked. Figure 8 shows the bed profiles of the tested condition N.1, obtained in two different runs at selected instants. At a defined instant the two profiles are almost coincident in the upstream slope of the scour cavity and in the dune downstream. Main differences can be identified as the maximum value of the scour depth and the downstream position where the scour cavity ends ($y = 0$). The evaluation of the repeatability was quantified by means of the root mean square (*rms*) of the standard deviations of the profiles in relation to their mean profile (not represented) at each instant (Table 2). The correlation coefficient between each two runs was also determined (R^2).

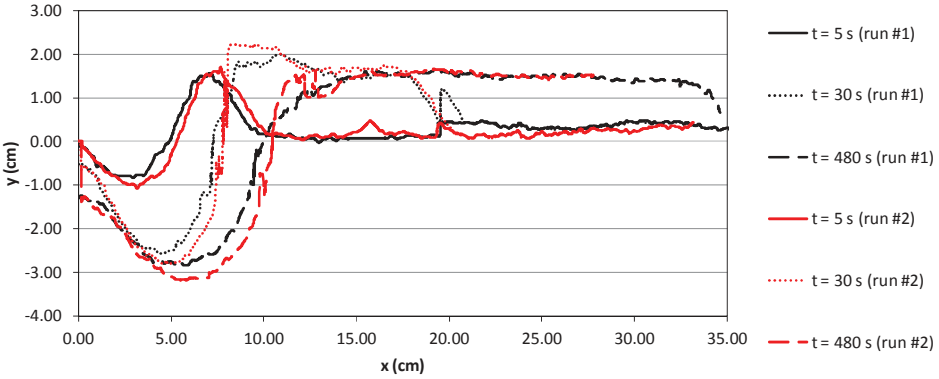

Fig. 8. Comparison of the sediment bed profiles in case of test condition N.1, for two different runs.

Table 2. Repeatability quantification in case of condition N.1

t (s)	R^2	rms (cm)
5	0.962	0.097
30	0.989	0.155
480	0.992	0.179

The obtained correlation coefficients indicate that both profiles are well correlated, especially at the end of the experiment (t = 480 s). The rms estimation suggests that the resolution of the profiles varies between 0.1 and 0.18 cm, values smaller than the

dimension of the glass spheres. In fact, the resolution of the measurements cannot be higher than the dimension of the sediments, reason why the repeatability of the experiments can be considered satisfactory.

3.2. Scour hole slopes

The upstream slope of the scour cavity, corresponding to the angle α (Figure 1) slightly increases during all the experiment (Figure 5) and reaches a maximum value as presented in Table 3. The angle β (Figure 1), measure of the scour cavity downstream slope, increases during the experiments until maximum values between 21º and 75º for flow conditions N.3 and N. 2 respectively. These angles vary accordingly with the flow conditions. For experiments without an apron (N.1 and N.2), the upstream slope is higher than the value observed for L = 8 cm (N.3 and N.4). For fixed apron length, the downstream slope is higher in case of higher tailwater depth, and the scour cavity is shorter (Figure 9). In case of flow conditions N.1 and N.2 the angle β is higher than the natural repose angle of glass spheres, equal to 25.5º in case of a dry sample [8]. This is an explanation why the glass spheres slide down upstream into the scour cavity and are once again transported up this slope by turbulent eddies, until they slide down again in a continuous cycle.

Table 3. Angles between the bed of sediments and the initial sediment level, upstream (α) and downstream (β) the scour cavity and (Ω) in the lee face of the dune

N.	α (º)	β (º)	Ω (º)
1	34	53	26
2	32	75	28
3	19	21	27
4	19	33	27

The dune's lee face slope is almost constant for all the flow conditions, and similar to the natural repose angle of glass spheres. This is in accordance with the observation of the sediments sliding down the lee face of the dune during the experiments. This slope, measured by the angle Ω (Figure 1), is similar at all the observed instants.

3.3. Solid transport quantification

In the present flow, two sediment transport modes can be identified: the suspended load, responsible for the sediment transport out of the scour cavity and the bedload, responsible for the sediment transport over the dune crest and their deposit on the lee face of the dune. As the scour process develops, the suspended load diminishes, and bedload is observed in the downstream slope of the scour cavity.

Figure 9 shows the scour volume per unit width (Figure 9a) and the corresponding solid transport rate per unit width (Figure 9b), both estimated at different instants.

Results show that for flow conditions N.1 and N.2 the solid transport rate is maximum for t = 10 s. For conditions N.3 and N.4 the solid transport rate is maximum for t = 30 s and 25 s, respectively. These results show that in the absence of an apron, the jet issuing the sluice gate has energy that immediately erodes the scour cavity. In the case of L=8 cm, the jet has smaller energy and the erosion process is slower. For both conditions, the solid transport rate is maximum when the scour cavity has reached around 38% of its maximum depth. After t = 200 s, the scoured volume remains almost constant and the solid transport rate is negligible.

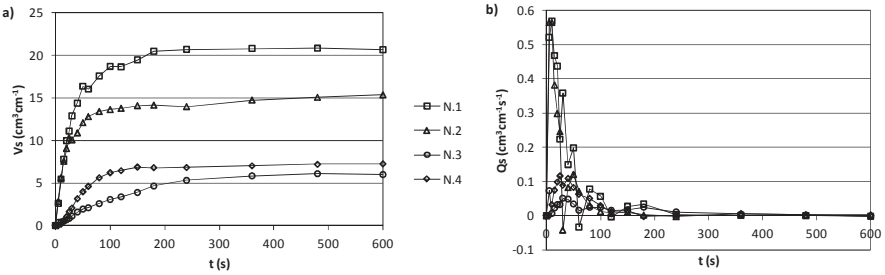

Fig. 9. Time evolution of the (a) scour volume per unit width and (b) solid transport rate per unit width.

4. Conclusion

The influence of the apron length and tailwater depth in the scour cavity and dune generated downstream of a sluice gate were analysed. The use of video recording and image processing allowed the definition of the bed morphology downstream the sluice gate. The repeatability of the experimental method developed was checked and considered to equal to a maximum value of the root mean square of the standard deviations of the profiles of 0.18 cm. The scour cavity maximum depth increased more rapidly for experiments without an apron and for smaller tailwater depths. The dune presented higher maximum height for experiments without an apron and for higher tailwater depths. Scour cavities with higher volumes corresponded to higher solid transport rates. About 200 s after the beginning of the experiments the solid transport rate was considered negligible.

More experimental tests are necessary to provide further insight into subjects such as the dune celerity and migration, as well as to propose a model for the sediment transport along the dune.

The authors thank Mr. João Rui Oliveira, technician of the Hydraulics Laboratory of the University of Minho, for his help with the experiments. This work was financially supported by: Project PTDC/ECM-HID/6387/2014 – POCI-01-0145-FEDER-016825 - funded by FEDER funds through COMPETE2020 - Programa Operacional Competitividade e Internacionalização (POCI) and by national funds through FCT - Fundação para a Ciência e a Tecnologia, I.P.

References

1. E.V. Richardson, S.R. Davies, *Evaluating Scour at Bridges, 4th Edition, Publication No. FHWA NHI 01-001 - Hydraulic Engineering Circular No. 18* (2001).
2. S. Dey, R.V. Raikar, J. Hydraul. Eng. **133(4)**, 399-413 (2007)
3. S. Dey, A Sarkar, J. Hydraul. Eng. **132(3),** 246-257 (2006)
4. G. Oliveto, W.H. Hager, J. Hydraul. Eng., DOI: 10.1061/(ASCE)HY.1943-7900.0000853 (2014)
5. B.W. Melville, *5th International Symposium on Hydraulic Structures. Hydraulic Structures and Society: Engineering Challenges and Extremes*, DOI: 10.14264/uql.2014.10 (2014)
6. B.W. Melville, S.-Y. Lim, J. Hydraul. Eng. **140(2)**, 149-155 (2013)
7. M. Aamir, Z. Ahmad, Phys. Fluids **28**, 105102 (2016)
8. J.R.G. Júnior. *Friction in granular materials, using glass spheres, Bachelor Monograpy*, University of Brasilia (in Portuguese) (2016)